

Anticancer Potential of Phytoconstituents Modulating Na⁺/K⁺ ATPase Pump; A Novel Repurposing Strategy

Suresh Kumar¹.M, Niladri Saha², Shyam Sundar³.P, Naresh⁴.P, Jubie^{5*}.S

¹TIFAC CORE in HD, JSS College of Pharmacy, JSS Academy of Higher Education and Research, Ooty, Nilgiris, 643001, Tamilnadu, India

²Department of Pharmaceutical Chemistry, JSS College of Pharmacy, JSS Academy of Higher Education and Research, Ooty, Nilgiris, 643001, Tamilnadu, India

Corresponding author: jubie@jssuni.edu.in.

Abstract

Repositioning the drugs through poly-pharmacological approaches, including cancer therapy is gaining scientific interest, as many non-cancer targeting drugs have well-established safety profile but unexplored for its potential to combat cancer. The complex heterotrimeric protein Na⁺/K⁺ ATPase (NKA) is complex. It is existing on the plasma membrane of eukaryotic cells and makes use of ATP for the maintenance of sodium and potassium transport. It has three subunits, α , β and γ . The α -subunit has four isoforms namely α 1, α 2, α 3, and α 4. One of the published studies reports that the α 1 subunit is over expressed and activated in certain malignancies like renal cell carcinoma, glioma, and melanoma. Thus, it is hypothesized that NKA has unique roles in cancer cell growth and development. For instance, Ouabain is a well-known inhibitor of NKA which is used primarily as a cardiac stimulant has also been recently reported for its potential anticancer properties in neuroblastoma cells. Consequently, the search for the molecules which has the potential to inhibit specific NKA in cancer cells gaining tremendous scientific attention. Recently perillyl alcohol has been reported for anticancer potential through NKA inhibition. Since perillyl alcohol has a cyclic ring in its structural frame, we opted the similar chemical signatures of Phyto terpenes and phytotannins of for our study. Thus, the present

study opted for scaffold repurposing strategy using *in-silico* methods to identify and screen some of the well-known phyto compounds for its possible anticancer effects by inhibiting NKA.

Keywords Repurposing, Phyto tannins, Phyto terpenes, perrilyl alcohol, Na K ATPase.

Introduction

Drug repositioning or drug repurposing is an approach is a way to deal with quickens the medication revelation process through the recognizable proof of a novel clinical use for a current medication affirmed for an alternate sign. A noteworthy issue of regular malignancy chemotherapy drugs (mainly DNA damaging agents) is famous symptoms that fundamentally decrease the quality existence of patients (1). As a large portion of non-malignant growth medications has pretty much nothing or decent reactions in humans, repositioning of non-disease drugs for anticancer treatment is viewed as a promising methodology for future anticancer medication improvement. Reliable with this view, a couple of those non-malignant growth medications are as of now under clinical examinations (for example Itraconazole, Nelfinavir, Digoxin, Riluzole, Mycophenolic corrosive and Disulfiram) against an assortment of human cancers (2, 3). Furthermore, drug repositioning altogether lessens the investigational time and cost. In

these lines, the structural frameworks of the old drugs rise as an extraordinary fortune trove for cancer therapy. This platform repurposing approach gives another importance on the familiar axiom of “to begin with an old drug” (4).

Sodium, potassium-activated adenosine triphosphatase (NKA) is a membrane-associated protein complex in creature cells that couples the vitality put away in ATP atoms to the vehicle of Na⁺ and K⁺ crosswise over cell layers at the expense of ATP, and thus maintains sodium and potassium homeostasis in animal cells. Also, to its function in maintaining cell homeostasis, NKA activity plays a crucial role in the function of neurotransmitter transporters essential for regulating neurotransmitter signaling and homeostasis. It is comprised of three subunits, α , β and γ . The α -subunit is made out of four isoforms to be specific $\alpha 1$, $\alpha 2$, $\alpha 3$, and $\alpha 4$ (5). The cardiovascular effects of NKA are well-reported; however, the emerging shreds of evidence indicate that NKA also acts as tumor invasiveness, metastasis, and tissue fibrosis, kidney cancer, prostate cancer, and signal transducers in cancer cells. This began from an investigation that ladies of breast cancer with cardio glycosides medicine have demonstrated a low death rate. Confirmations state that the NKA essentially adjust the physiological occasions of beginning times of tumorigenesis. Moreover, the changes in the NKA activity during the early stages of tumorigenesis was observed to be pre-existing, even before morphological proof can exhibit the nearness of tumors. Of note, a few trial and clinical investigations showed that cardiovascular glycosides inspire anticancer agents. Together recommending that NKA go about as a potential target for a new anticancer agent (6). The significance of NKA in anticancer treatment has likewise been proposed utilizing mixes inconsequential to the heart glycoside structure, for example, the monoterpene perillyl alcohol (POH) (**Figure 1**) is found in essential oils from different plants that have chemo preventive and chemotherapeutic exercises against various tumors, including glioblastomas (GBM), the

most widely recognized and dangerous human cerebrum tumors. Because of the huge job of anticancer action of perillyl alcohol through the restraint of NKA, the present work centers around the investigation of anticancer potential phytoterpenes and phytotannins through the inhibition of NKA action. The phytotannins and phytoterpenes have been selected for the presence of perillyl alcohol alike scaffold in their chemical structure.

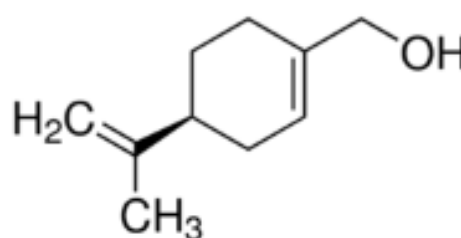


Figure 1. Chemical Structure of Perillyl alcohol

Materials and Methods

Selection of phytoconstituents and target

A library of forty-three phyto terpenes and Phyto tannins were chosen for the investigation. The α -subunit of Na⁺/K⁺ATPase with Ouabain (PDB id: 3A3Y) was picked for our investigation.

In-silico ADMET profile:

Procedure: In-silico Absorption, Distribution, Metabolism, Excretion, and Toxicity of all the 43 compounds were performed by utilizing the QikProp (v5.3) simulation module of Schrödinger. It helped in anticipating both the physically critical descriptors and pharmaceutically important properties. Different parameters such as octanol/water and water/gas log Ps, log S, log BB, overall CNS activity, Caco-2, and MDCK cell permeabilities, log K_{hsa} for human serum albumin binding and log IC₅₀ for HERG K⁺-channel blockage and total solvent accessible surface area (SASA) were determined. All compounds were neutralized before being utilized by QikProp (v5.3). The Phytoconstituents were additionally assessed for adequacy of the inhibitors dependent on the

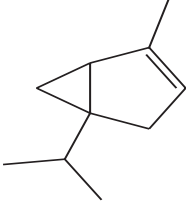
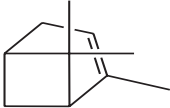
Lipinski's standard.

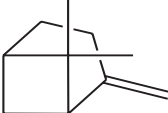
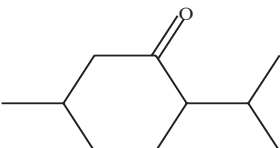
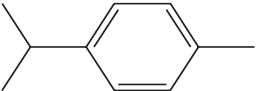
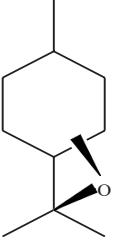
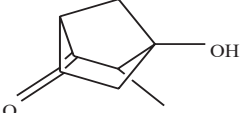
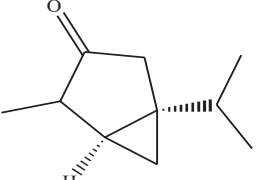
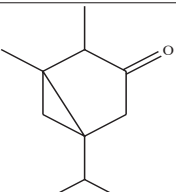
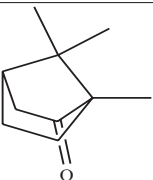
Molecular docking and protein preparation

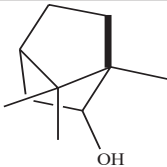
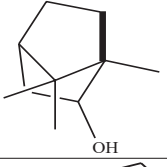
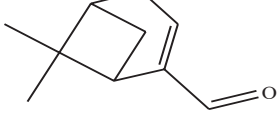
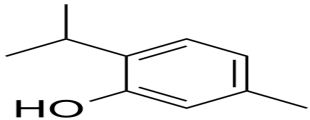
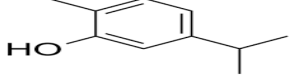
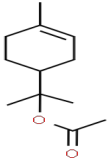
Protocol: A library of forty-three phyto terpenes and phytotannins (**Table 1**) has been sketched using Chem Sketch programming 8.0. The 3D structures of ligands were retrieved in mol format in Maestro v 11.3 and the ligands were optimized utilizing ligprep (4.3) module (Schrödinger 2018-1). The generated energetically minimized conformers and the chirality and ionization state has been retained by Epik (4.1). By using Optimized Potentials for Liquid Simulations (OPLS-3) force field for the prepared ligands minimization. This force field has been designed especially for small molecule simulation. The X-ray crystal structure of the NKA receptor [PDB ID: 3A3Y] was taken from the protein data bank (www.rcsb.org) having a resolution of 2.8 Å has been selected for receptor-target. The crystal structure consists of A, B, and G chain having amino acids of 1028, 305, and 74 respectively. Chain A is the α -subunit, bound with Ouabain, potassium, and magnesium ion. Whereas chain B and G are β -subunit and Phospholemman-like protein bound with cholesterol and N-acetyl-glucosamine in chain B. From the literature survey, the α -subunit of the receptor has been kept and the remaining chains have been deleted. The protein has been prepared using the protein preparation wizard. The crystallographic inhibitor and ions (K^+ and Mg^+) were kept and the unwanted water molecules have been deleted. The protonation at $pH\ 7.0 \pm 2.0$ and the assignment of the bond

orders have been done. The missing atoms of the side chains and the breaks present were added and repaired using prime. The hydrogen of the altered species has been minimized using PROKA at $pH\ 7.0$. The root means square of the heavy atoms has been converged to 0.30 Å by minimizing restrained energy using a full atomic model with the OPLS-3 force field. The Ramachandran plot was produced which uncovered that the vast majority of the amino acids and non-glycin residues (97.8%) were in the most favorable region (**Figure 3**). The centroid center of the Ouabain binding area of the receptor has been used for 3D grid box (10Å) generation for the preparation of binding pocket. The van-der Waals radius scaling for the receptor has been kept default. The scaling factor has been kept 1.0 and the partial charge cutoff has been kept 0.25. No constraints and flexibility of the rotatable group have not kept during grid generation. And no excluded volume has been included in the grid generation. The docking study has been done by glide (v7.5) module using those prepared ligands. The docking has been performed in extra-precision mode (XP) without using any constraint in ligand and receptor. A Sampling of the ligand has been kept flexible and also sample nitrogen inversion and sample ring conformation have been kept as default. Penalty for nonplanar conformation of amide group has been counted. And also no torsional constraints for the hydroxyl group have been kept. Then the docking has been performed. Then the docking model has been validated by docking the co-crystal ligand Ouabain in the same receptor binding pocket.

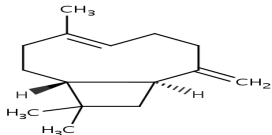
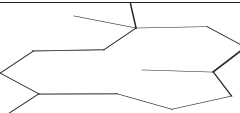
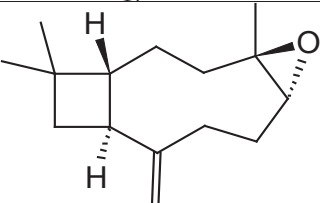
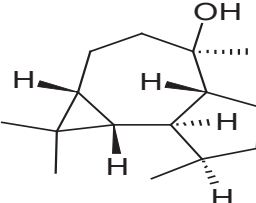
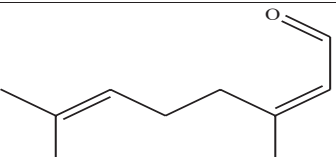
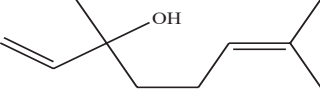
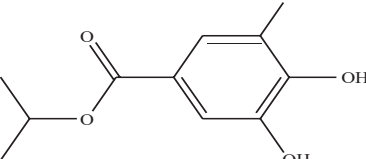
Table 1. Selected Phytoconstituents for the study

S.No	Name of the Phytoconstituent	Chemical Structure
1.	α -Thujone	
2.	α -Pinene	

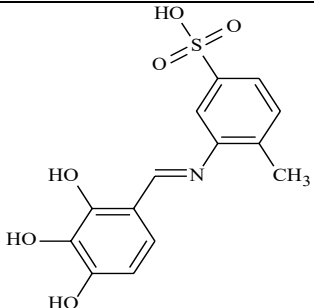
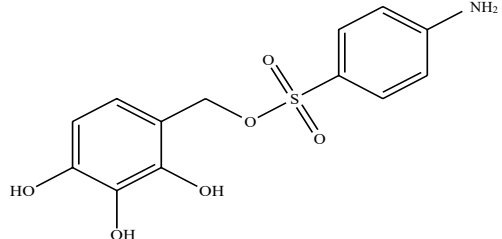
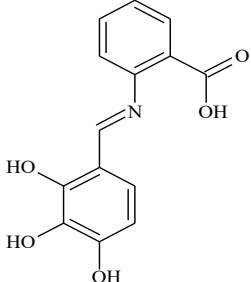
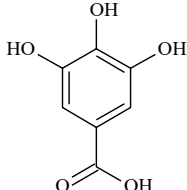
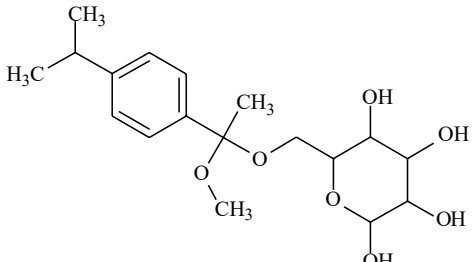
3.	Camphene	
4.	β -Pinene	
5.	Menthone	
6.	p -Cymene	
7.	1,8-cineole	
8.	Camphenilone	
9.	<i>Cis</i> -Thujone	
10.	<i>Trans</i> -Thujone	
11.	Camphor	

12.	Borneol	
13.	Isoborneol	
14.	Myrtenal	
15.	α -Terpineol	
16.	Linalyl acetate	
17.	Bornyl acetate	
18.	Thymol	
19.	Carvacrol	
20.	α -Terpenyl acetate	

Anticancer potential of phytoconstituents

21	E- β -Caryophyllene	
22	α -Humulene	
24.	β -Caryophyllene oxide	
25.	Viridiflorol	
26.	Citral	
27.	Linalool	
28.	Menthol	
29.	Limonene	
30.	Isopropyl gallate	

31.	n-butyl gallate	
32.	2,3-dihydroxy-5-carboxyphenoxy acetic acid	
33.	Methyl 2,3-dihydroxy-5-carbomethoxyphenoxy acetate	
34.	3,4,5-trihydroxybenzoyl glycolamide	
35.	3-benzoyl gallic acid	
36.	3,5-dibenzoyl gallic acid	
37.	2,3-dihydroxyphenoxy acetic acid	
38.	Methyl 2,3-dihydroxyphenoxy acetate	

39.	2,3,4-trihydroxybenzylidene-2'-methyl-5'-sulfo aniline	
40.	2,3,4-trihydroxybenzyl sulfanilic acid	
41.	2,3,4-trihydroxybenzylidene-anthranilic acid	
42.	Gallic acid	
43.	[6-(ethoxymethyl)-tetrahydro-2H-pyran-2,3,4,5-tetraol	

MMGBSA binding energy studies

The strength of these Phytoconstituents having a high docking score (the best 14) has been kept for Molecular Mechanics-Generalized Born Surface Area (MM-GBSA) (Schrödinger 2018-1) based free energy calculation. This module has been used to determine the free binding energy of the ligands. The docked receptor-ligand complex has been taken and the minimization of these complexes has been done by local optimization feature in prime (v4.8). Then without applying any constraints on flexible residues the VSGB 2.0 energy model has been used for simulation. It is a physics-based correction for hydrophobic interaction, π - π interactions, self-contact interaction, and hydrogen bonding and it is also a poses an optimized implicit solvation model. Using the OPLS-3 force-field the energy of those complexes has been carried out.

Results and Discussion

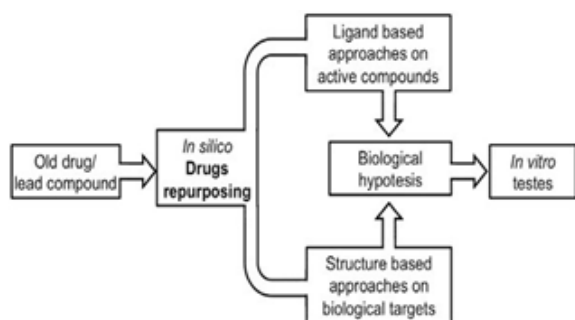


Figure 2: Overview of in-silico drug repurposing

The accessibility of a few set up clinical drug libraries and fast propels in infection science, genomics and bioinformatics have quickened the pace of both movement and *in-silico* drug repositioning. In activity-based drug repositioning, real drugs might be required for screening. Interestingly, *in-silico* drug repositioning uses open information bases and bioinformatics instruments to efficiently distinguish collaboration arranges among drugs and protein targets. Having a bunch

measure of data on the structure of proteins and pharmacophores, this methodology has been broadly utilized for drug repositioning. The accessibility of a few built-up clinical drug libraries and rapid advances in disease biology, genomics, and bioinformatics has quickened the pace of both activity and *in-silico* drug repositioning (7-9).

We adopted the scaffold repurposing strategy through *in-silico* tools for our study. The forty- three Phytoconstituents as selected scaffolds towards the target have been repurposed for the target The *in-silico* docking studies and binding free energy calculations were performed by the modules Glide (v7.6 ;) and Prime (v4.9) of Schrödinger (2017-3)3(Maestro v11.3) individually. The catalytic pockets of target protein NKA α were produced and analyzed utilizing the site map device. The protein was readied utilizing protein preparation wizard; crystallographic water atoms (water particles without H bonds) were erased. Prime was utilized for including all missing side-chain residues and to manufacture breaks present in the structure. Hydrogen bonds comparing to pH 7.0 were included considering the proper ionization states for both the acidic and fundamental amino acid residue. The approval of the docking system had been performed by figuring of RMSD between the co-crystal posture

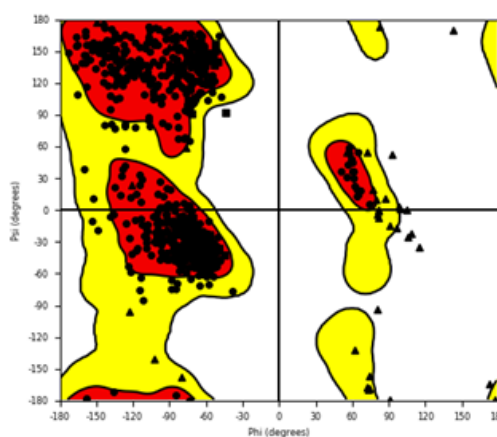


Table 3. Binding free energy calculation using Prime/MM-GBSA approach

of native ligand and the redocked posture of the native ligand. The redocked native ligand and co-crystallized structure were superimposed and the RMSD was seen as 0.9205 Å. Their superimposition was likewise accurately repeated inside the binding domain of the target receptor. It splendidly coordinated the way that RMSD between the co-crystallized posture of native ligand and the redocked posture of native ligand ought not to surpass 2 angstroms as can be valued. The Ramachandran plot for NKA was created and every one of the amino acid residues was in the favored region (**Figure 3**).

Molecular docking was performed to clarify the binding mode capability of NKA and forty-three Phytoconstituents. The planned Phytoconstituents were docked alongside the co-crystal Ouabain which filled in as reference

G-scores above -7 were chosen for further binding energy studies and the outcomes were delineated in (**Table 2**). The phenolic compound 2, 3-dihydroxy-5-carboxy phenoxy acetic acid was positioned as top scorer.

There were significant nonbonding interactions observed for compound 2,3,4-trihydroxybenzylidene-sulfanilic acid than the standard Ouabain. The hydroxyl groups present in the Ouabain exhibited strong hydrogen bonds with the amino acid residues GLY 326, ASN 129, and THY 804 respectively. Similarly, the two hydroxyl groups of the compound exhibited strong hydrogen bond interactions with the negatively charged amino acid residue GLH 786 and the third hydroxyl group had hydrogen bonding with the amino acid residue GLY 326. Interestingly, the phenyl

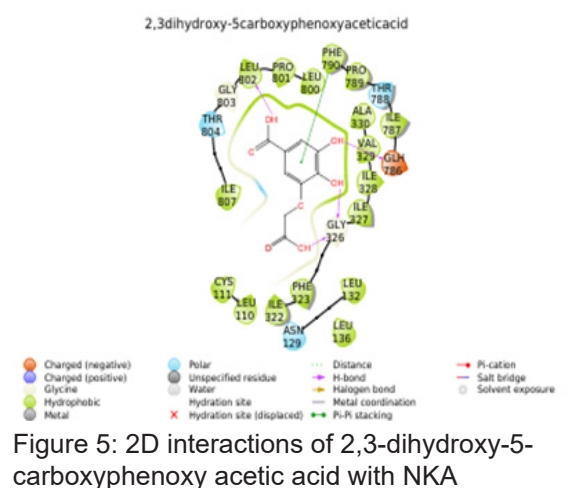
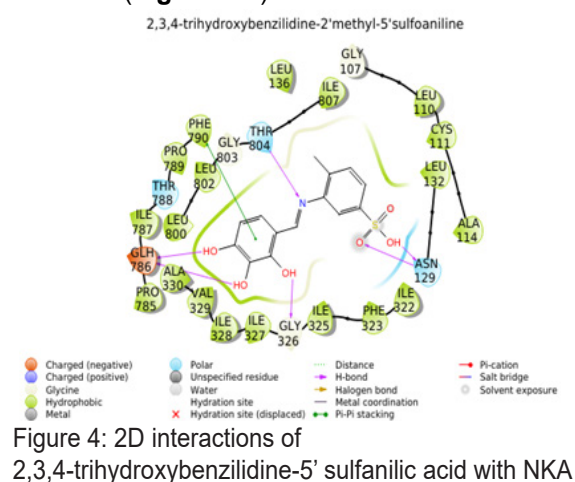
Table 2: Docking data of Phytoconstituents

S. No	Name of the Compound	G-Score	Lipophilic EvdW	HBond	LowMW
1	2,3,4-trihydroxybenzylidene-2-methyl-5-sulfoaniline	-8.67	-4.724	-3.36	-0.422
2	2,3,4-trihydroxybenzylidene-1-anthranilic acid	-9.39	-4.09	-3.364	-0.5
3	Ouabain	-7.36	-4.651	-4.32	0
4	2,3-dihydroxyphenoxyacetic acid	-7.32	-2.99	-3.515	-0.5
5	Gallic acid	-7.46	-2.379	-3.757	-0.5
6	2,3-dihydroxy-5-carboxy phenoxy acetic acid	-10.11	-2.61	-3.592	-0.5
7	3 benzoyl gallic acid	-9.11	-3.063	-3.131	-0.5
8	3,4,5-trihydroxybenzoyl glycolamide	-7.42	-2.894	-3.346	-0.5
9	n-butylgallate	-7.46	-3.858	-2.676	-0.5
10	2,3,4-trihydroxybenzylsulfanilic acid	-8.59	-3.22	-3.571	-0.469
11	Methyl-2,3-dihydroxyphenoxyacetate	-7.10	-3.025	-2.024	-0.5
12	3,5-dibenzoyl gallic acid	-8.54	-4.976	-1.096	-0.239
13	Methyl 2,3-dihydroxy-5-carboxy methoxy phenoxyacetate	-7.41	-3.332	-1.367	-0.5
14	6-(ethoxymethyl)-tetrahydro-2H-pyran-2,3,4,5-tetraol	-8.43	-4.854	-2.88	-0.312

standard also. The G-scores were utilized to look at the relative binding affinities of the structured Phytoconstituents against the protein NKA. The G score of Ouabain is -7 and it was kept as cut off point. Among the forty three Phytoconstituents, the fourteen Phytoconstituents which had

ring of the compound exhibited strong π - π stacking with the amino acid PHE 790 and the imine nitrogen had a stronger hydrogen bond interaction with the polar amino acid THY 804. The same kind of interactions was observed for the second compound 2, 3-dihydroxy-5-carboxy

phenoxy acetic acid. Though the hydrogen bond interactions of the selected Phytoconstituents are similar to the standard, the π - π stacking with the hydrophobic PHE 790 may be the reason for more binding affinity and less binding energy for the compound. These non-covalent interactions Van der Waals, columbic interaction, π - π interaction, and hydrogen interactions of the two compounds and the standard Ouabain were shown in (Figure 4-6).



To gauge the better binding strength and binding free energy, MM-GBSA measure had additionally been completed for the top fourteen G-scorers and the outcomes were delineated in (Table 3). It was apparent from

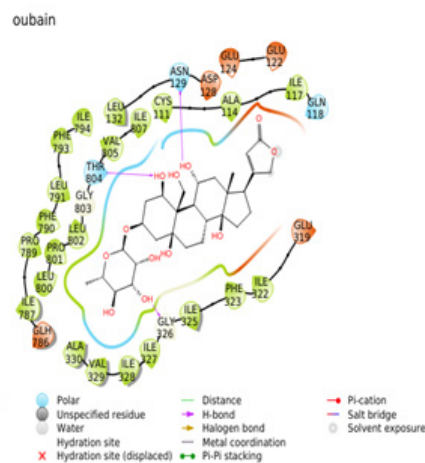


Figure 6: 2D interactions of Ouabain with NKA

the examination, that the van der Waals ($\Delta G_{\text{bindvdW}}$) and coulomb energy interactions were major great contributors. The Van der Waals and Coulomb energy interactions in docked complexes changed between -11.76 to -41.15 and between -4.33 to -83.64 kcal/mol plainly expressed the inclination of the van der Waals and Coulomb energy interaction components. Be that as it may, the best binding energy ΔG -104.11 kcal/mol was found for the compound 2,3,4-trihydroxybenzilidene-5'sulfanilic acid, which additionally demonstrated a higher coulomb energy term (-84.64 kcal/mol) and a great Van der Waals force (-41.02 kcal/mol). Another compound 2, 3-dihydroxy-5-carboxy phenoxy acetic acid had the second most astounding binding energy (-102.54) showed ideal Van der Waals contribution (-32.81 kcal/mol) and strong ideal Coulomb energy term (-50.41 kcal/mol). Comparable outcomes were watched for different mixes too. It was reasoned that the coulomb energy term is the main impetus for ligand binding. The outcomes have all around corresponded with the past investigation that indicated non-polar columbic interactions were the supporters for the binding efficiency into the catalytic pocket of the receptor.

All the selected Phytoconstituents had fitting log P (octanol/water) value for biological efficacy with zero to one Lipinski infringement. They

Table 3: Binding free energy calculation using Prime/MM-GBSA approach

S. No	Compound code	ΔG_{bind} (Kcal/mol)	ΔG_{bind} Coulomb	ΔG_{bind} Vander	ΔG_{bind} HBond	ΔG_{bind} covalent	ΔG_{bind} Lipophilic
1	2,3,4-trihydroxybenzylsulfanilic acid	-72.29	-50.97	-13.66	-3.75	8.43	-20.16
2	2,3,4-trihydroxybenzylidene-1-anthranilic acid	-77.83	-60.98	-14.72	-1.37	-7.08	-14.41
3	Ouabain	-61.44	-38.1	-29.33	-3.78	8.99	-18.45
4	2,3-dihydroxyphenoxyacetic acid	-102.54	-50.41	-32.37	-4.57	19.98	-14.34
5	Galic acid	-74.15	-60.45	-32.82	-6.92	22.01	-20.32
6	2,3-dihydroxy-5-carboxy phenoxy acetic acid	-56.78	-64.28	12.24	2.08	-14.43	-8.82
7	3 benzoyl gallic acid	-25.41	-27.45	-12.26	1.27	-14.93	-6.69
8	3,4,5-trihydroxybenzoyl glycolamide	-49.74	-35.14	-22.48	-8.5	24.02	-12.96
9	n-butylgallate	-74.83	-82.28	-41.15	-7.88	21.71	-25.37
10	2,3,4-trihydroxybenzylidene-2-methyl-5'-sulfoaniline	-104.11	-83.64	-16.17	-1.19	3.98	-16.66
11	Methyl-2,3 dihydroxyphenoxyacetate	-50.61	-4.33	-11.76	0.97	-15.91	-10.8
12	3,5 dibenzoyl gallic acid	-77.28	-13.81	-25.65	-0.48	-1.11	-19.92
13	Methyl 2,3-dihydroxy-5-carboxy phenoxyacetate	-29.79	-16.83	-25.6	0.5	-4.71	-13.65
14	6-(ethoxymethyl)-tetrahydro-2H-pyran-2,3,4,5-tetraol	-42.32	-49.25	-18.68	-2.81	24.15	-18.97

Table 4: Predictions of ADMET for compounds by QIKPROP 3.4

S. No	Compound code	CNS	Mol. Wt	Dipole	SASA	Volume	Donor HB	Accept HB	QP log poct
1.	2,3,4-trihydroxybenzylidene-2-methyl-5'-sulfoaniline	-2	226.23	2.02	495.40	797.31	3	4.25	13.62
2.	2,3,4-trihydroxybenzylideneanthranilic acid	-2	228.158	2.63	426.24	685.321	4	6.25	15.50
3.	Ouabain	-2	256.23	1.83	526.47	849.26	2	6.25	14.18
4.	2,3-dihydroxyphenoxy acetic acid	-2	227.17	5.66	443.24	707.40	5	6.75	18.04
5.	Galic acid	-2	274.22	2.90	515.38	848.93	3	6	17.00
6.	2,3-dihydroxy-5-carboxy phenoxy acetic acid	-2	378.33	6.49	685.87	1169.09	2	7.75	21.77
7.	3 benzoyl gallic acid	-2	184.14	2.32	383.29	602.11	3	4.25	11.86
8.	3,4,5-trihydroxybenzoyl glycolamide	-2	198.17	2.29	433.33	683.53	2	4.25	11.22
9.	n-butylgallate	-2	323.32	9.47	564.38	953.16	4	7.25	20.79
10.	2,3,4-trihydroxybenzylidene-2-methyl-5'-sulfoaniline	-2	309.29	9.50	542.96	899.86	4	7.25	20.38

11.	Methyl-2,3-dihydroxyphenoxyacetate	-2	273.24	4.81	503.29	841.81	4	5.25	17.62
12.	3,5 dibenzoyl gallicacid	-2	584.65	6.49	766.33	1549.37	8	18.1	38.63
13.	Methyl 2,3-dihydroxy-5- carbo methoxy phenoxyacetate	-2	170.12	3.69	343.19	528.07	4	4.25	12.80
14.	6-(ethoxymethyl)-tetrahydro-2H-pyran-2,3,4,5-tetraol	-2	356.41	2.370	644.01	1150.89	4	10	22.13
Recommended Values		-2 to +2	130 - 725	1 -12.5	300 - 1000	500 - 2000	0 – 6	2-20	8- 35

likewise had fulfilling pharmacological properties of 95% accessible drugs with high to medium anticipated oral absorption availability with no lethal usefulness. The molecular weight of every ligand was inside the range of 170 to 584 with Log S esteems inside the satisfactory range of 95% of existing drugs (**Table 4**).

Conclusion

Scaffold repurposing strategy through *in-silico* tools was adopted for the identification of lead molecules. The NKA has a significant role in the induction of apoptosis and autophagy. Since, perillyl alcohol, a phytoperpene has proven for anticancer activity through the inhibition of NKA, we selected the phytoterpenes and phytotannins possessing similar chemical signatures. To check our hypothesis, theoretical *in-silico* studies have been carried out. Compared to the phytoterpenes, the phytotannins exhibited a significant binding affinity towards NKA, shown by the docking results and MMGBSA results. Two compounds namely 2,3,4-trihydroxy benzylidene-2'-methyl-5'sulfoaniline and 2,3-dihydroxyphenoxy acetic acid were proposed for further bio-assay characterization including cytotoxic potential on various cancer cells. Nonetheless, our study for the first time screened the selected phytoterpenes and phytotannins for their potential to bind/modulate NKA activity. Further *in-vitro* screening against cancer cell lines and enzyme inhibition studies

are in advancement in our research facility. The recognized compounds might be repositioned for cancer therapy through the hindrance of Na⁺/K⁺ ATPase after intensive preclinical and clinical examinations.

References

1. Issa, N.T., Kruger, j., Byers, S.W. and Dakshanamurthy, S. (2013). Drug repurposing a reality: from computers to the clinic. *Expert Review of Clinical Pharmacology*, 6 (2): 95–97. Doi: 10.1586/ecp.12.79.
2. Chong, C.R., Xu, J., Lu, J., Bhatt, S., Sullivan, D.J. and Liu, J.O. (2007). Inhibition of Angiogenesis by the Antifungal Drug Itraconazole. *ACS Chemical Biology*, 2 (4): 263–270. Doi: 10.1021/cb600362d.
3. Xie, L., Evangelidis, T., Xie, L. and Bourne, P.E. (2011). Drug Discovery Using Chemical Systems Biology: Weak Inhibition of Multiple Kinases May Contribute to the Anti-Cancer Effect of Nelfinavir. *PLoS Computational Biology*. 7 (4): e1002037. Doi: 10.1371/journal.pcbi.1002037.
4. Chen, H., Wu, J., Gao, Y., Chen, H. and Zhou, J. (2016). Scaffold Repurposing of Old Drugs Towards New Cancer Drug Discovery. *Current Topics in Medicinal Chemistry*, 16 (19): 2107–2114. Doi: 10.217

7. Huang, R., Southall, N., Wang, Y., Yasgar, A., Shinn, P., Jadhav, A., Nguyen, D.T. and Austin, C.P. (2011). The NCGC Pharmaceutical Collection: A Comprehensive Resource of Clinically Approved Drugs Enabling Repurposing and Chemical Genomics. *Sci. Transl. Med*, 3 (80): 16.
8. Dakshanamurthy, S., Issa, N.T., Assenia, S., Seshasayee, A., Peters, O.J., Madhavan, S., Uren, A., Brown, M.L. and Byers, S.W. (2012). Predicting New Indications for Approved Drugs Using a Proteochemometric Method', *Journal of Medicinal Chemistry*, 55 (15): 6832–6848. Doi: 10.1021/jm300576q.
9. Karasneh, R. A., Murray, L. J. and Cardwell, C. R. (2017). Cardiac glycosides and breast cancer risk: A systematic review and meta-analysis of observational studies: Cardiac glycosides and breast cancer risk', *International Journal of Cancer*, 140 (5): 1035–1041. Doi: 10.1002/ijc.30520.